Scripta Materialia 135 (2017) 119–124

Contents lists available at ScienceDirect

Scripta Materialia

journal homepage: www.elsevier.com/locate/scriptamat

Viewpoint paper

Building digital twins of 3D printing machines☆

T. DebRoy [a,*], W. Zhang [b], J. Turner [c], S.S. Babu [d]

[a] The Pennsylvania State University, University Park, PA, United States
[b] The Ohio State University, Columbus, OH, United States
[c] Oak Ridge National Laboratory, Oak Ridge, TN, United States
[d] University of Tennessee, Knoxville, TN, United States

ARTICLE INFO

Article history:
Received 18 August 2016
Received in revised form 29 November 2016
Accepted 3 December 2016
Available online 19 December 2016

Keywords:
Additive manufacturing
Microstructure and properties
Heat transfer and material flow
Solidification and texture
Residual stresses and distortion

ABSTRACT

Geometrical conformity, microstructure and properties of additively manufactured (AM) components are affected by the desired geometry and many process variables within given machines. Building structurally sound parts with good mechanical properties by trial and error is time-consuming and expensive. Today's computationally-efficient, high-fidelity models can simulate the most important factors that affect the AM products' properties, and upon validation can serve as components of digital twins of 3D printing machines. Here we provide a perspective of the current status and research needs for the main building blocks of a first generation digital twin of AM from the viewpoints of researchers from several organizations.

1. Introduction

Microstructure and mechanical properties of additively manufactured (AM) components are affected by many process variables such as the heat source power, power distribution, scanning speed, powder/wire feed rate, hatch spacing and substrate preheat [1,2]. Building structurally sound components with good mechanical properties based solely on experiments is time-consuming and expensive due to the need for numerous experiments with various combinations of process variables [3–5]. An alternative is to synthesize the available knowledge base of AM and welding to build a digital replica of the AM hardware. The digital twin needs to integrate the major physical components of the evolution of microstructure and properties into a tractable numerical framework: energy interaction with powders, heating and cooling rates, solidification parameters, phase transformation kinetics, evolution of residual stresses and distortion, and defects [6,7]. The visual abstract shows the anatomy of such a digital twin in more details.

There are many advantages of building a digital twin such as (i) minimizing expensive trial and error optimization to save time and money, (ii) shortening the path for product qualification, and (iii) reducing/alleviating defects. The goal of the current viewpoint paper is to examine the current status and research needs for the building blocks of a digital twin: (a) heat and material flow simulation, (b) simulation of solidification, grain structure and texture evolution, (c) modeling of microstructure and properties, and (d) calculations of residual stresses and distortion. Note that this article is not intended to provide a comprehensive review of all existing computational models, rather the authors' view of the components necessary to build a first generation digital twin for AM systems.

2. Modeling of heat transfer - the foundation for understanding structure and properties

Modeling of heat transfer and material flow can provide the transient temperature fields, heating and cooling rates, solidification parameters and the dominant heat flow directions [3,6]. These quantities are critical for the prediction of structure and properties, texture, residual stresses, distortion and many types of defects [2]. Both the temperature field in the entire part and the flow conditions in the liquid metal pool must be calculated by solving the equations of conservation of mass, momentum, energy in transient three-dimensional form with appropriate boundary conditions [3,4,8]. A comparison of numerical techniques commonly used for the heat transfer calculations is summarized in Table 1.

The computational domain is divided into small control volumes or cells, and it changes with time as the part is built layer upon layer. At

☆ This manuscript has been authored by UT-Battelle, LLC, under Contract No. DE-AC05-00OR22725 with the U.S. Department of Energy. The United States Government retains and the publisher, by accepting the article for publication, acknowledges that the United States Government retains a non-exclusive, paid-up, irrevocable, world-wide license to publish or reproduce the published form of this manuscript, or allow others to do so, for United States Government purposes.

* Corresponding author.
E-mail address: debroy@psu.edu (T. DebRoy).

http://dx.doi.org/10.1016/j.scriptamat.2016.12.005
1359-6462/

Table 1
A comparison of commonly used techniques for the modeling of heat transfer in additive manufacturing.

Method	Selected features	References
Finite element method (FEM)	Widely used, computationally efficient, can accommodate large and complex computational domains, but ignores convective heat transfer	[16,55]
Finite difference method (FDM)	Computationally efficient but less so than FEM for large and complex domains, meso-scale, and widely used for transient heat and fluid flow calculations	[3,4]
Level set method (LSM)	Computationally intensive, meso-scale, tracks free surface profile of melt pool, but tends to suffer from non-conservation of mass	[17]
Volume of fluid (VOF) method with FDM	Computationally intensive, meso-scale, tracks free surface geometry with mass conservation maintained but at less sharp interface than LSM	[19,20]
Lattice Boltzmann method (LBM) and Arbitrary Lagrangian-Eulerian (ALE)	Most computationally intensive but suitable for massively parallel computing, meso-scale, capable of tracking detailed melting of individual powder particles using VOF	LBM [18] and ALE [6]

any given time, all cells are assigned temperature dependent thermophysical properties of either a solid, powder, liquid or gas. At every time step the properties of the cells change because of changes in the material of the cell and/or its temperature. The governing equations are discretized into algebraic equations which are solved by an appropriate technique to obtain enthalpies (temperatures), and three components of liquid alloy velocities [3,4].

Fig. 1(a) shows the typical computed temperatures and velocities in the liquid pool [3]. The results show large velocities of liquid alloy in a small melt pool in the range of 400–600 mm/s [3] driven by the spatial gradient of temperature [9]. These large velocities indicate convective heat transfer as the main mechanism of heat transfer within the liquid pool during AM [3–5,8,9]. Fig. 1(b) shows the computed thermal cycles at the mid-height and mid-length of the alternate layers in a nine-layer structure [3]. In each of these cycles, the first peak corresponds to a position of the laser beam just above the monitoring location and the subsequent peaks occur during the deposition of the subsequent layers. Fig. 1(c) shows that the calculated cooling rate for a laser directed energy deposition of AISI stainless steel (SS) 316 agrees well with the experimental data [10]. Higher heat input results in somewhat slower cooling because of the larger size of the melt pool.

Moreover, the temperature gradient, G, and the solidification growth rate, R, provide useful information about the evolution of solidification structure [11,12]. In particular, the local cooling rate (G·R) is related to the scale of microstructure and G/R influences the morphology of the solidification front [12]. Higher G/R indicates a higher tendency for plane front solidification. The effect of heat input [13] on the ratio G/R is shown in Fig. 1(d). Among different engineering alloys, the temperature gradient in the melt pool is the smallest with Inconel® Alloy 718 (IN 718) deposits followed by that for Ti-6Al-4V and SS 316 alloy deposits [14]. As a result, the SS 316 deposits exhibit the highest G/R followed by that of Ti-6Al-4V and IN 718 alloy deposits.

Various simplifications are used to make the heat and fluid flow calculations tractable [3]. They include two-dimensional approximations [15] and three dimensional calculations ignoring convective heat transfer [16] and three-dimensional convective calculations assuming a flat top surface [3,4]. As shown in Table 1, efforts have also been made to model the free surface profile by either the level-set method [17] or

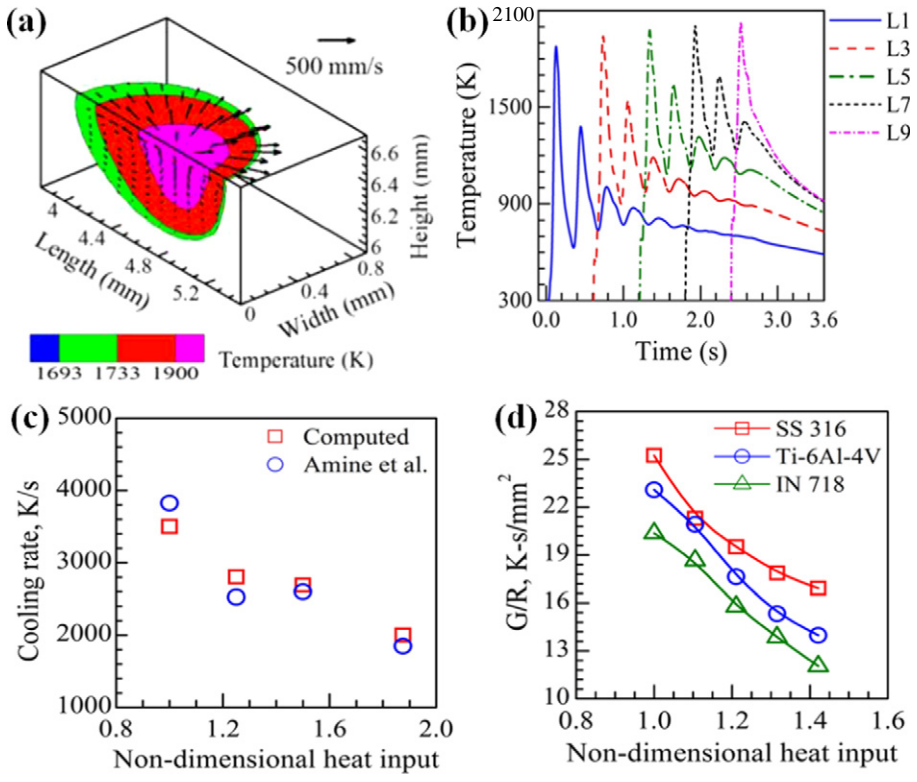

Fig. 1. (a) Computed temperature and velocity fields during laser directed energy deposition AM [3]. (b) Computed thermal cycles during AM [3]. (c) A comparison of the experimental [10] and computed cooling rates [3]. (d) Computed G/R values for the AM of three common alloys [13]. The non-dimensional heat input is defined as the ratio of laser power by the scanning speed divided by the ratio of reference laser power to the reference scanning speed. It provides a measure of the energy deposited per unit length of the deposit.

by the volume of fluid (VOF) method [19,20]. In addition, powder bed systems are sensitive to both feedstock properties and interaction between the energy input (whether laser or electron beam) and powder particles. Extensive efforts are underway to predict the transients including powder redistribution due to recoil pressures and formation of balling defects [6,7]. It is interesting to note the similarity of these processes with keyhole formation during traditional laser welding [20].

The above methods are starting to be utilized for the calculations of microstructure and residual stresses and distortion, as discussed in the following sections. However, these methods are computationally intensive, and have not yet been used for closed-loop process control. One potential way to use these results is to create a database of results and develop reduced-order models through approaches such as neural networks [21]. This surrogate modeling approach has been used for automation and controls required for closed-loop proportional-integral-derivative (PID) controller for increased stability in laser metal wire deposition [22]. In addition, we anticipate an increased use of physically-accurate models even within the control loop due to a combination of three factors. First, continued improvement in computational efficiency through improved solvers and preconditioners and adaptive methods. Second, increased computational power within AM machines themselves, similar to what has happened in medical imaging technology over the past decade and what is now happening in vehicle technology (not just for engine performance but also for situational awareness for driver assistance and ultimately autonomous vehicles). Finally, robust high-bandwidth networks that increasingly allow for the possibility of cloud-based clusters with hundreds or thousands of processors to help determine build-specific process parameters.

3. Solidification modeling

Heat transfer modeling not only provides a good understanding of the solidification morphology and the scale of solidification microstructure, but also serves as a basis for customizing solidification texture which is important for mechanical and chemical properties and performance of components [11,23]. Many of the physical processes that occur during metal additive manufacturing processes [2] are similar to those in welding [3], which involve melting and solidification under temperature gradients and gyrations [24]. Therefore, we can leverage the well-published knowledge related to prediction of weld metal solidification [25,26] and solid-state transformations [27] under single and multi-pass conditions [28], as well as static and dynamic mechanical properties [29–33].

Classic work by Kurz et al. [34] provides a strong foundation for predicting rapid solidification. For example, texture development in single-crystal welds was demonstrated by Gaumann et al. [35]. A detailed analysis of solidification texture for IN 718 fabricated by laser directed energy deposition process has been studied by Wei et al. [11]. Striking differences in solidification textures due to the influence of local temperature fields resulting from different scanning patterns have been clearly demonstrated. Particularly, solidification texture depends on the local heat flow directions and competitive grain growth in one of several preferred growth directions depending on the crystal structure of the alloy [11]. For unidirectional laser scanning, primary dendrite orientation of about 60° with the horizontal plane (Fig. 2(a) and (b)) was calculated from the numerical model and also observed from experiments for all depositing layers [11]. During bidirectional laser scanning (Fig. 2(c) and (d)), the angle between primary dendrites of neighboring layers was about 90° [11]. The heat transfer calculations considering the molten pool fluid flow helped to understand the mechanism of formation of the solidification texture for both cases and provide a basis for customizing solidification textures during AM. Finally, the same concepts have been extended to complex melt boundary conditions imposed by electron beam melting (EBM) AM by Dehoff et al. [36] and Raghavan et al. [37]. With these tools, the researchers have demonstrated the ability to induce site-specific microstructures within a given geometry manufactured by the EBM process. This provides the direction for AM achieving targeted properties within a given geometry without relying on complex secondary processes.

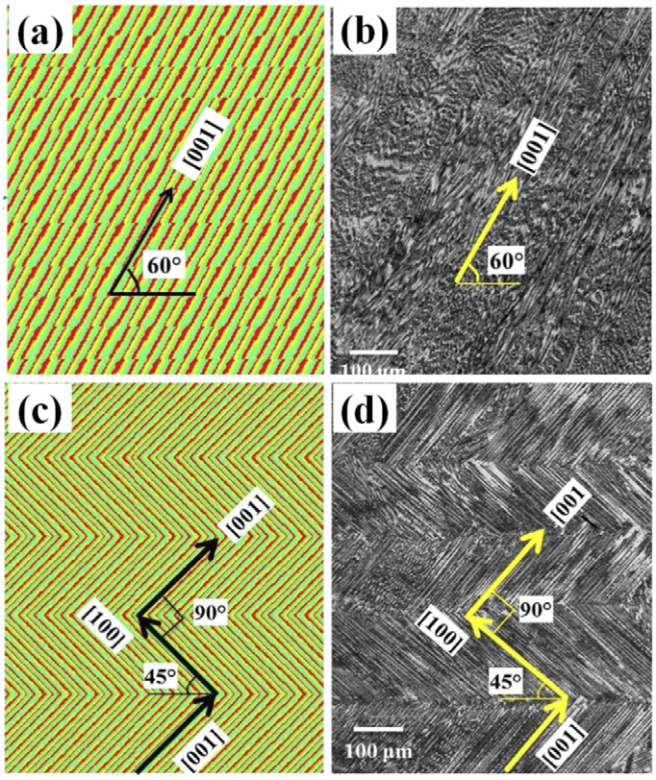

Fig. 2. (a) Calculated solidification patterns of primary dendrites for unidirectional laser scanning where laser scanning directions are same for the deposition of all layers. (b) Optical micrograph of the as-deposited IN 718 sample for unidirectional laser scanning. (c) Calculated solidification patterns of primary dendrites for bidirectional laser scanning where the scanning direction alternates in successive layers. (d) Optical micrograph of the as-deposited IN 718 sample for bidirectional laser scanning [11]. All results are for laser directed energy deposition.

4. Prediction of microstructure and properties

Prediction of the solid-state transformations that occur during hundreds or thousands of thermal cycles during the layer-by-layer building process is an important component of a digital twin. Kelly and Kempe [38] correlated the temperature gyrations to a banded microstructure in Ti-6Al-4V deposits and suggested that a homogeneous microstructure could be obtained by manipulating thermal cycles. Chaudhary et al. [39] have reviewed the approaches to predict these thermal cycles as well as approaches to use the same for microstructure control. Makiewicz et al. [40] used thermal models to help select process parameters to maintain the whole build above the β-transus temperature of Ti-6Al-4V. On cooling from this high temperature, the whole build region underwent solid-state decomposition to basketweave microstructure. Subsequently the same researchers developed a material model that is capable of predicting the evolution of different morphologies including grain-boundary, colony, and basketweave $\alpha + \beta$ microstructures based on a simultaneous transformation kinetics framework [41]. These modeling techniques can be extended to predicting the microstructure that evolves during solid-state precipitations of nickel alloys that experience complex thermal cycling. For example, a rapid build made on IN 718 substrate showed soft areas on the top regions compared to the bottom regions. This was rationalized by calculating the fractions of γ' and γ'' precipitates (see Fig. 3) as a function of thermal cycles at different locations [42]. These variations are quite sensitive to the geometry, process parameters and scan strategies [36,38].

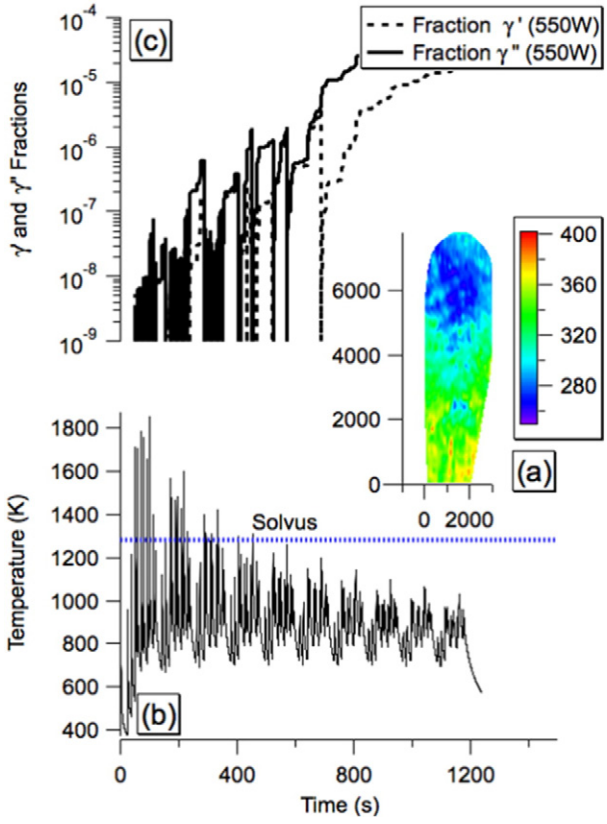

Fig. 3. (a) Microhardness map showing severe mechanical heterogeneity as a function of build height. The top regions are softer compared to the bottom regions. Typical (b) thermal cycle and (c) precipitate fraction show the complex dissolution and growth of both γ′ and γ″ precipitates [40,42].

The literature [43–45] on prediction of properties (e.g., hardness, yield strength, tensile strength, strain hardening exponent, crack growth under fatigue or impact loading, creep rupture properties) of welds based on microstructure, through semi-empirical to detailed physical modeling, is extensive. In principle, the above sub-models can be extended to additive manufacturing with calibration. It is essential to consider the presence of physical defects in predicting the performance of additively manufactured components. Recently, Prabhu et al. [46] showed that even with uniform basketweave microstructure the fatigue life of Ti-6Al-4V builds made by laser directed energy deposition depended on defects such as porosity and lack of fusion. Thus there is a need to couple the microstructure and property models with models for defect formation [47].

5. Modeling of residual stresses and distortion

Residual stresses and distortion originate from spatially non-uniform heating and cooling cycles. The key physical phenomena include heat transfer and stress equilibrium (solid mechanics) [48–51]. It is noted that the temperature distribution can be significantly influenced by convection within the molten pool, as discussed earlier. However, given its complexity, the molten metal flow phenomenon is often ignored when solving the thermal-stress problem.

Numerical modeling of residual stresses and distortion in AM is typically based on the sequentially-coupled analysis [52], where the temperature field is solved first. The temperature field as a function of time is then imported into the stress model as "thermal loads" to calculate the reaction stresses and strains. Fully-coupled models solve the heat conduction and stress equilibrium equations simultaneously [53] and require substantially more computational resources. Most models are formulated as a quasi-static problem (as opposite to a dynamic problem) since the speed of stress wave in metals is of several orders of magnitude faster than that of heat conduction. In other words, whenever a new temperature field is established, the stress and strain fields are redistributed "instantaneously" to reach a new static equilibrium state. The finite element method (FEM) with a Lagrangian mesh that deforms with the material is commonly used, but other approaches (e.g. particle methods) are also possible.

Simulation of the entire part is essential to accurately calculate the residual stresses and distortion. The large number of layers and passes within a single layer sometimes make it impractical to simulate the individual passes for building a full-sized part. For computational efficiency a lumped method, where successive melting passes and even successive layers are grouped together, is often utilized. The choice of lumped vs. individual pass approaches influences two important aspects of modeling of AM systems: material deposition and heat input from energy beam.

First, to account for material deposition, a mesh for the entire part is created. The bead is often simplified to have a rectangular cross section. With a Lagrangian mesh, the so-called (1) element birth and (2) quiet element are the two commonly used methods for handling material deposition [16,49]. For the former, elements for the yet to be deposited material are inactivated at the beginning and then gradually activated (or born) along the build path. For the latter, all elements are present at the beginning and assigned to arbitrary or powder properties so that their presence does not affect the temperature and stresses of the already deposited material. The properties for those quiet elements are then gradually switched to the physical properties based on the build path. The individual pass approach can be computationally affordable for directed energy deposition AM with a relatively small number of passes [16]. On the other hand, power bed based AM has many melting layers and passes, for which several successive layers are typically lumped together with elements for those layers being activated at once [2].

Second, for describing the heat input a surface or volumetric heat flux centered at the energy beam is used in the individual pass approach [48,49]. The position of the heat flux center is updated based on the deposition path, thus representing a moving heat source. For the lumped pass approach, a stationary heat flux is assigned to the lumped region over a user-specified time period.

The aforementioned thermal-stress modeling approach is applicable to both powder blown (and wire feed) and powder bed AM processes. However, the use of powder feedstock in powder bed AM process requires some special treatments. For instance, Fig. 4(a) shows the calculated temperature distribution during laser directed energy deposition (or blown powder) AM [49] where the mesh covered only the solid metal. On the other hand, Fig. 4(b) shows the normal stress distribution in laser powder bed based AM where the mesh included both the consolidated and powder phases [54]. The model considered phase-dependent material properties (e.g., thermal conductivity) and a volumetric contraction from the melting consolidation of powder particles [48,54]. Other recent developments for computational efficiency include the integrated multi-scale models [55,56]. Particularly, Li et al. [56] proposed an interesting method that maps the local residual stress field calculated in the meso-scale layer hatch model to the macro-part model for fast prediction of part distortion. However, the validity of such an approach for complex part geometry is yet to be demonstrated.

Finally, many thermal-stress models for AM are developed by customizing or enhancing general-purpose multi-physics finite element codes available either commercially or through research institutions. Commercial codes include 3DSim (http://3dsim.com/), ESI (http://www.esi-group.com/), Additive Works (https://additive.works/), Abaqus (http://www.3ds.com/) and Ansys (http://www.ansys.com/), while research codes include Diablo from Lawrence Livermore National Laboratory. Depending on the code, additional user customizations for AM simulation vary from simply defining material properties and

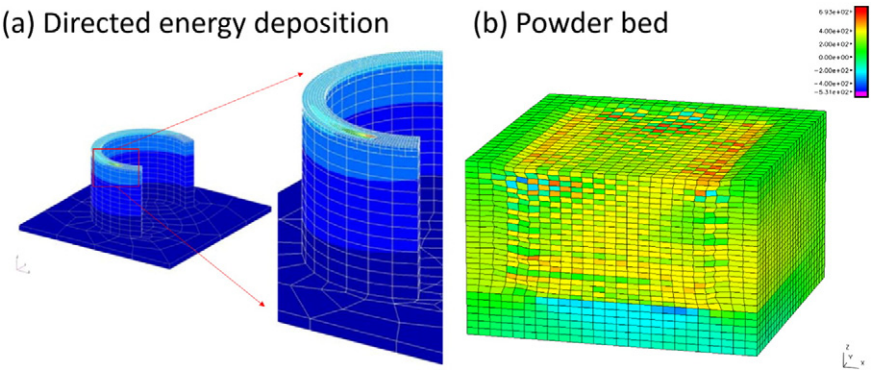

Fig. 4. (a) Calculated temperature distribution for directed energy deposition [49]. (b) Normal stress for laser powder bed after 12 layers deposited [54].

build paths, to applying the appropriate loading conditions for thermal heat input, element activation scheme, and constitutive relationships (especially high-temperature stress-strain curves).

6. Current status and research needs

The components required to construct a digital twin of AM hardware are still developing and much work is still needed for its completion. However, examples of recent progress provided in this paper indicate that construction of a first generation digital twin is within the reach of the AM research community. Considerable efforts are needed for the synthesis of the various component models to construct the integrated digital twin, its testing, and validation with experiments. The digital twin is not intended to replace experiments. However, it will help to reduce the total number of experiments needed for part qualification, minimize defects and provide structurally sound, reliable parts. Several research needs will have to be addressed to achieve this goal.

An important requirement is a database of temperature dependent thermophysical properties for commonly used engineering alloys. Mechanical properties are needed at high temperatures typically for low strain rate. Control of component texture is a unique feature of AM. Development of solidification texture must be quantitatively studied based on solidification and phase transformation principles. Multi-scale models must be developed to investigate the grain growth and subgrain structure for various alloys. To accurately obtain site-specific microstructures from solidification and solid-state transformation it is necessary to couple the microstructure and property models with models for defect formation, because physical defects are important for estimating the properties of the AM components. Computationally efficient models for predicting residual stresses and distortion must be scalable to full size parts with complex geometry. Models need to consider volumetric change during solid state phase transformation, transformation induced plasticity and creep strain. Given the increasing number of commercial and research codes for thermal-stress modeling of AM, a set of benchmarking problems will be valuable to assess the accuracy and speed of different codes. Finally, these advanced numerical models are often inappropriate for real time applications and need to be used to construct reduced-order models to facilitate real time calculations.

The tangible demonstrations of predicting temperature, defect, microstructure, and residual stresses and distortion prompt the following question: is it possible to design alloys specifically for the unique thermal and stress signatures of a given additive manufacturing process to achieve targeted properties and allow for minimal qualification testing? Building a digital twin of AM hardware holistically integrating models for temperature, microstructure and properties, and residual stresses and distortion that further consider defects would be helpful to answer this and similar important questions.

Acknowledgements

We acknowledge the support from the RAMPUP program of the U.S. Department of Energy (DOE) through Oak Ridge National Laboratory (ORNL). One of the authors acknowledges helpful discussions with H. L. Wei and T. Mukherjee of Penn State University. Part of the research discussed in this article was sponsored by DOE Office of Energy Efficiency and Renewable Energy, Advanced Manufacturing Office, under Contract DE-AC05-000R22725 with UT-Battelle, LLC, and by the Laboratory Directed Research and Development Program of ORNL, managed by UT-Battelle, LLC.

References

[1] D.D. Gu, W. Meiners, K. Wissenbach, R. Poprawe, Int. Mater. Rev. 57 (2012) 133–164.
[2] W.J. Sames, F.A. List, S. Pannala, R.R. Dehoff, S.S. Babu, Int. Mater. Rev. 61 (2016) 315–360.
[3] V. Manvatkar, A. De, T. DebRoy, J. Appl. Phys. 116 (2014) 124905.
[4] V. Manvatkar, A. De, T. DebRoy, Mater. Sci. Technol. 31 (2015) 924–930.
[5] A. Raghavan, H.L. Wei, T.A. Palmer, T. DebRoy, J. Laser Appl. 25 (2013) 052006.
[6] S.A. Khairallah, A.T. Anderson, A. Rubenchik, W.E. King, Acta Mater. 108 (2016) 36–45.
[7] M. Matthews, G. Guss, S.A. Khairallah, A.M. Rubenchik, P.J. Depond, W.E. King, Acta Mater. 114 (2016) 33–42.
[8] T. Debroy, S.A. David, Rev. Mod. Phys. 67 (1995) 85–112.
[9] S.A. David, T. Debroy, Science 257 (1992) 497–502.
[10] T. Amine, J.W. Newkirk, F. Liou, Appl. Therm. Eng. 73 (2014) 500–511.
[11] H.L. Wei, J. Mazumder, T. DebRoy, Sci. Rep. 5 (2015) 16446.
[12] H.L. Wei, J.W. Elmer, T. DebRoy, Acta Mater. 115 (2016) 123–131.
[13] T. Mukherjee, V. Manvatkar, A. De and T. DebRoy, Unpublished research (2016).
[14] T. Mukherjee, J.S. Zuback, A. De, T. DebRoy, Sci. Rep. 6 (2016) 19717.
[15] S. Morville, M. Carin, P. Peyre, M. Gharbi, D. Carron, P. Le Masson, et al., J. Laser Appl. 24 (2012) 032008.
[16] P. Michaleris, Finite Elem. Anal. Des. 86 (2014) 51–60.
[17] X. He, J. Mazumder, J. Appl. Phys. 101 (2007) 053113.
[18] C. Körner, E. Attar, P. Heinl, J. Mater. Process. Technol. 211 (2011) 978–987.
[19] Y.S. Lee, W. Zhang, Addit. Manuf. (2016)http://dx.doi.org/10.1016/j.addma.2016.05.003.
[20] J.Y. Lee, S.H. Ko, D.F. Farson, C.D. Yoo, Phys. D. Appl. Phys. 35 (2002) 1570–1576.
[21] V.D. Manvatkar, A. Arora, A. De, T. DebRoy, Sci. Technol. Weld. Join. 17 (2012) 460–466.
[22] A. Heralic, A.-K. Christiansson, M. Ottosson, B. Lennartson, Opt. Lasers Eng. 48 (2010) 478–485.
[23] Z.Q. Wang, T.A. Palmer, A.M. Beese, Acta Mater. 110 (2016) 226–235.
[24] S.S. Babu, Int. Mater. Rev. 54 (2009) 333–367.
[25] S.A. David, J.M. Vitek, Int. Mater. Rev. 34 (1989) 213–245.
[26] D. Dye, O. Hunziker, R.C. Reed, Acta Mater. 49 (2001) 683–697.
[27] J.S. Kirkaldy, Scand. J. Metall. 20 (1991) 50–61.
[28] R.C. Reed, H.K.D.H. Bhadeshia, Acta Metall. Mater. 42 (1994) 3663–3678.
[29] H.K.D.H. Bhadeshia, ISIJ Int. 39 (1999) 966–979.
[30] J.C. Ion, K.E. Easterling, M.F. Ashby, Acta Metall. 32 (1984) 1949–1962.
[31] H.T. Kang, P.S. Dong, J.K. Hong, Int. J. Fatigue 29 (2007) 1546–1553.
[32] D.F. Watt, L. Coon, M. Bibby, J. Goldak, C. Henwood, Acta Metall. 36 (1988) 3029–3035.
[33] Y.P. Yang, S.S. Babu, F. Orth, W. Peterson, Sci. Technol. Weld. Join. 13 (2008) 232–239.
[34] W. Kurz, B. Giovanola, R. Trivedi, Acta Metall. 34 (1986) 823–830.
[35] M. Gaumann, C. Bezencon, P. Canalis, W. Kurz, Acta Mater. 49 (2001) 1051–1062.

[36] R.R. Dehoff, M.M. Kirka, W.J. Sames, H. Bilheux, A.S. Tremsin, L.E. Lowe, et al., Mater. Sci. Technol. 31 (2015) 931–938.
[37] N. Raghavan, R. Dehoff, S. Pannala, S. Simunovic, M. Kirka, J. Turner, et al., Acta Mater. 112 (2016) 303–314.
[38] S.M. Kelly, S.L. Kampe, Metall. Mater. Trans. A Phys. Metall. Mater. Sci. 35A (2004) 1861–1867.
[39] A. Chaudhary, et al., ASM Handbook, 22B, 2010 240–252.
[40] K. Makiewicz, S.S. Babu, M. Keller, A. Chaudhary, Trends in Welding Research: Proceedings of the 9th International Conference 2013, pp. 970–977.
[41] S.J. Jones, H.K.D.H. Bhadeshia, Metall. Mater. Trans. A Phys. Metall. Mater. Sci. 28 (1997) 2005–2013.
[42] S. S. Babu, Proceedings of the International Conference on Solid-Solid Phase Transformations in Inorganic Materials 2015, Jun 28-July 3, 2015, Eds. M. Millitzer, G. Botton, L-Q. Chen, J. How, C. Sinclair and H. Zurob, TMS, pp. 1019–1026
[43] A. Simar, Y. Brechet, D. de Meester, A. Denquin, C. Gallais, T. Pardoen, Prog. Mater. Sci. 57 (2012) 95–183.
[44] O. Grong, H.R. Shercliff, Prog. Mater. Sci. 47 (2002) 163–282.
[45] S. S. Babu, “Introduction to integrated weld modeling,” ASM Handbook, Vol. 22B, Edited D. U. Furrer and S. L. Semiatin, ASM International, 2010
[46] A.W. Prabhu, T. Vincent, A. Chaudhary, W. Zhang, S.S. Babu, Sci. Technol. Weld. Join. 20 (2015) 659–669.
[47] P.S. Wei, J. Heat Transf.-Trans. ASME 133 (2011) 031005.
[48] W. King, A.T. Anderson, R.M. Ferencz, N.E. Hodge, C. Kamath, S.A. Khairallah, Mater. Sci. Technol. 31 (2015) 957–968.
[49] R. Martukanitz, P. Michaleris, T. Palmer, T. DebRoy, Z.-K. Liu, R. Otis, et al., Addit. Manuf. 1-4 (2014) 52–63.
[50] T. Mukherjee, W. Zhang, T. DebRoy, Comput. Mater. Sci. 126 (2017) 360–372.
[51] T. Mukherjee, V. Manvatkar, A. De, T. DebRoy, Scr. Mater. 127 (2017) 79–83.
[52] P. Farahmand, R. Kovacevic, Opt. Laser Technol. 63 (2014) 154–168.
[53] J. Cao, M.A. Gharghouri, P. Nash, J. Mater. Process. Technol. 237 (2016) 409–419.
[54] N.E. Hodge, R.M. Ferencz, J.M. Solberg, Comput. Mech. 54 (2014) 33–51.
[55] D. Pal, N. Patil, K. Zeng, B. Stucker, J. Manuf. Sci. E. T. ASME 136 (2014).
[56] C. Li, C.H. Fu, Y.B. Guo, F.Z. Fang, J. Mater. Process. Technol. 229 (2016) 703–712.